INT. J. NUM. METH. HEAT FLUID FLOW, VOL. 2, 271–279 (1992)

FINITE ELEMENT ANALYSIS OF A PARTITIONED CAVITY UNDER MIXED THERMAL CONDITIONS

P. K. GHOSH, A. SARKAR AND V. M. K. SASTRI

Indian Institute of Technology, Madras 600 036, India

ABSTRACT

Natural convection in a square cavity with a centrally located partition is considered. While one of the side walls is fully active, the other is partly insulated. Numerical simulation, based on the finite element method, has been carried out for different lengths of the active surface. The results have been compared with the cases when the cavity is without partition as well as the case of a partitioned cavity with fully active side walls.

KEY WORDS Finite element analysis Partitioned cavity Natural convection

INTRODUCTION

Buoyancy-induced flows abound in nature as well as numerous other areas of practical interest. Increasingly, intensive study in the past two decades has further clarified the conceptual understanding of many fundamental aspects. While the initial researches concentrated mostly on external natural convection, the trends have now shifted to other classes of equally important convection phenomena; for example, natural convection in enclosed spaces, double-diffusive convection, combination of free and forced convection. Analysis of natural convection in enclosed spaces is difficult due to the fact that, unlike in the external natural convection, the core is surrounded completely by the wall boundary layers. The problem was initially identified by Ostrach[1] and, as yet, understanding of the problem is incomplete. The fundamental configuration used in the study of internal natural convection consists of a differentially heated square cavity. A broader classification of this problem depends on the interaction between the imposed temperature gradient and the gravity vector, i.e., whether they are parallel or perpendicular to each other. Both these cases have been extensively studied. In fact, the one in which the imposed temperature gradient is perpendicular to the gravity vector is so extensively studied that it is considered now as a bench-mark solution[2] and is used for effective comparison with the newly-developed algorithms. Effects of Prandtl number, aspect ratio and inclination were studied. The motivation behind these studies stems from several important application areas such as double pane windows, solar collector devices etc. The continued diversification of the application areas needed more research in this field with newer boundary conditions. In the last few years, attention has been focused on cavities with 'partially active side-walls'. Its application areas include thermal design of buildings, spread of fire in enclosed spaces etc. By partially active side walls it is implied that either or both the side walls are partly insulated and partly under isothermal boundary conditions. This gives rise to flux-singularity. The singular point in question, refers to the point at which the transition from isothermal to adiabatic boundary condition occurs. Poulikakos[3] considered the convection in a square cavity in which one vertical wall contained both warm and cold regions. He investigated the effects of changing the positions of

0961–5539/92/030271–09$2.00

Received March 1991
Revised December 1991

hot and cold plates and concluded that the situation yields an interesting variety of natural convection flows which can lead to complete or incomplete thermal penetration depending on the relative position of the heated and cooled portions along the side wall. November and Nansteel[4] studied the convection in a cavity which is cooled from the side and subjected to partial heating from below. They reported results relating to the variation of the length of the zone of partial heating and concluded that the convection heat transfer plays the most significant role when slightly less than half of the lower surface is heated. Valencia *et al.*[5] investigated numerically the heat transfer in square cavities with partially active vertical side walls. They concluded that the circulation depends strongly on the exit length downstream of the active zones but heat transfer depends less on this parameter. They also presented flow structures for five different relative positions of the active zones. The present authors in an earlier work[6] considered a broad range of situations in which the effect of mixed thermal conditions were considered on the side walls as well as the bottom wall. With water as the working fluid, they were able to obtain excellent agreement with that of Reference 4 as far as the flow structure is concerned. They concluded that the Prandtl number has an important effect on the orientation of the flow within the cavity. In another study[7], the present authors numerically investigated the flow patterns and heat transfer in cavities when one of the side walls is subjected to mixed conditions while the other was left under isothermal conditions. In all, six different cases have been considered by them. They also compared these results with the conventional differentially heated square cavity with fully active side walls. In the present work, a square cavity with a centrally located partition has been considered. While the cold wall is left fully active, the hot wall on the left hand side (*Figure 1*) is subjected to mixed thermal conditions. The present problem then relates to two different classes of problems. Before proceeding further, a brief review of the class of problems relating to conjugate natural convection seems to be relevant. Conjugate problems seem to have been taken up first by Sparrow and Prakash[8] who considered natural convection in a square enclosure of which one vertical wall is cooled by an external natural convection boundary-layer flow. They concluded that the Nusselt numbers, under such circumstances, are 60% of those for the standard enclosure. Results have also been reported for cavities separated by a single or multiple partitions[9–11]. Effect of inclination has also been studied[10]. The present authors, in one of their earlier works[12], carried out an extensive numerical study regarding the effect of aspect ratio and effect of shifting the partition from the central position of the cavity. They concluded that, in general, the effect of introducing a partition, when centrally located, reduces heat transfer by about 50% when compared with the cavity without a partition. They also noted that when the partition is shifted slightly from the central position to either side, the effect on heat transfer is only marginal.

Figure 1 describes the physical situation along with the boundary conditions and gives results with emphasis on flow structure and heat transfer for cases in which XH assumes values of 0.25, 0.5 and 0.75. The Prandtl number is held at unity while the Ra_H is varied from 10^3 to 10^6.

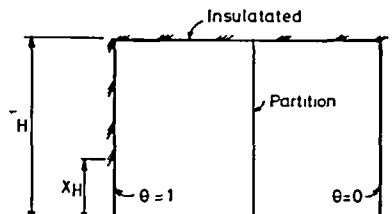

Figure 1 Physical and computational domain

GOVERNING EQUATIONS

Assuming steady, two-dimensional incompressible laminar flow the conservation equations may be written as follows:

$$\frac{\partial u}{\partial x}+\frac{\partial v}{\partial y}=\theta \tag{1a}$$

$$u\frac{\partial u}{\partial x}+v\frac{\partial u}{\partial y}=-\frac{1}{\rho}\frac{\partial p}{\partial x}+\nu\left(\frac{\partial^2 u}{\partial x^2}+\frac{\partial^2 u}{\partial y^2}\right) \tag{1b}$$

$$u\frac{\partial v}{\partial x}+v\frac{\partial u}{\partial y}=-\frac{1}{\rho}\frac{\partial p}{\partial y}+\nu\left(\frac{\partial^2 v}{\partial x^2}+\frac{\partial^2 v}{\partial y^2}\right)+\beta.g.(T-T_C) \tag{1c}$$

$$u\frac{\partial T}{\partial x}+v\frac{\partial T}{\partial y}=\alpha\left(\frac{\partial^2 T}{\partial x^2}+\frac{\partial^2 T}{\partial y^2}\right) \tag{1d}$$

The fluid is assumed to be Newtonian and the Boussinesq approximation is valid. The same fluid is assumed to occupy both the containers.

On introduction of the following non-dimensional quantities, $U=u/u_0$; $V=v/u_0$; $\theta=(T-T_C)/(T_W-T_C)$; $X=x/H$; $Y=y/H$ and $P=p/(\rho.u_0^2)$ the governing equations take the following form:

$$\frac{\partial U}{\partial X}+\frac{\partial V}{\partial Y}=0 \tag{2a}$$

$$U\frac{\partial U}{\partial X}+V\frac{\partial U}{\partial Y}=-\frac{\partial P}{\partial X}+\frac{1}{A}\left(\frac{\partial^2 U}{\partial X^2}+\frac{\partial^2 U}{\partial Y^2}\right) \tag{2b}$$

$$U\frac{\partial V}{\partial X}+V\frac{\partial V}{\partial Y}=-\frac{\partial P}{\partial Y}+\frac{1}{A}\left(\frac{\partial^2 V}{\partial X^2}+\frac{\partial^2 V}{\partial Y^2}\right)+\theta \tag{2c}$$

$$U\frac{\partial \theta}{\partial X}+V\frac{\partial \theta}{\partial Y}=\frac{1}{A.Pr}\left(\frac{\partial^2 \theta}{\partial X^2}+\frac{\partial^2 \theta}{\partial Y^2}\right) \tag{2d}$$

where $A=\sqrt{Gr_H}$ and $u_0=\sqrt{\beta.g.H(T_H-T_C)}$

The choice of the expression for u_0 is dictated by the fact that this seems to be more reasonable while the other choices, as $u_0=\alpha/H$ or ν/H may lead to incorrect decisions while scaling the flow.

FINITE ELEMENT FORMULATION

The finite element formulation of the aforesaid constitutive equations starts with defining the variables at the nodes of the element. The type of element used for the present work is an isoparametric eight-noded quadrilateral. While U, V, θ have been defined at all the nodes, the pressure has been defined only at the corner nodes, i.e. pressure is interpolated in a linear manner. Application of Galerkin's formulation scheme to the constitutive equations (2a)–(2d) leads to the following equations:

$$[F_1]^{(0)}=\int M^T(\nabla.\omega)\,ds^{(0)} \tag{3a}$$

$$[F_2]^{(0)}=\int N^T\left[\omega.(\nabla.\omega)+\nabla P-\frac{1}{A}(\nabla^2\omega)-\theta.Z\right]ds^{(0)} \tag{3b}$$

$$[F_3]^{(0)}=\int N^T\left[\omega.(\nabla\theta)-\frac{1}{A.Pr}(\nabla^2\theta)\right]ds^{(0)} \tag{3c}$$

where $\omega = U.i + V.i$ and z is a unit vector in the direction of the gravity. The weight functions, i.e. N^T and M^T denote the interpolating polynomials for (U, V, θ) and P respectively. $[F_1]^{(0)}$ $[F_2]^{(0)}$ $[F_3]^{(0)}$ are the residue matrices. Usually, the element based area integrals constitute the element stiffness matrix. However, for the Newton–Raphson method, the element stiffness matrix is based on the gradient of the right hand side of (3a)–(3c) with respect to the variables. So, the element stiffness matrix is also termed as a Jacobian matrix. The residue matrices (element-based) after being assembled globally form what are known as the forcing vectors. Now, the resulting system of linear simultaneous equations are solved by a frontal solver[13].

NUMERICAL SOLUTION PROCEDURE

The complexity of the numerical solution arises from the fact that the thermal conditions on the partition are not known *a priori*. So an iterative scheme needs to be employed. Initiation of the iterative scheme is done by assigning a uniform temperature along the partition wall. The constitutive equations are now solved for any one of the two chambers. Heat fluxes are then calculated at the partition wall. These nodal heat fluxes serve as boundary conditions for the other chamber. This is how thermal information is passed from one chamber to the other. Iterations are terminated when the biggest residue in each of the chambers reaches a pre-assigned value which is as low as 5×10^{-5}. The choice of this limit of convergence is, however, not arbitrary. It has been observed that when this datum is achieved, the interface temperature and heat flux values at the partition wall as well as the values of the variables in either of the chambers do not exceed by more than 0.01% in comparison with the values obtained in the earlier iteration. The details of the method have been described by the authors in Reference 12.

The mesh size plays a very important role in problems of this nature particularly when cavities with mixed thermal conditions are being studied. To ensure that the results are independent of the grid size, three meshes with non-uniform spacing were considered. When the results were compared for a 12×12 and 14×14 mesh sizes, the cold wall Nusselt number, which was considered as a basis of comparison, varied by about 1%. In the next phase, a 15×12 mesh was employed. This mesh had 15 elements; when the results of this mesh were compared with the 14×14 mesh, the cold wall Nusselt number did not show any change up to the fourth decimal place. The same effect was also observed in such quantities as the partition wall temperature and the x-component of the temperature gradient at the partition. Hence, the 15×12 mesh was selected for the present work. The same mesh size was used for both the cavities. In this mesh, the x-extent and y-extent for a typical corner node as well as the singular point were not allowed to exceed 0.002.

Regarding the treatment of singularity, a few words are in order. In the present work, mixed thermal conditions have been assigned only at the hot wall. Owing to the presence of the singularity, the heat flux distribution shows a tendency towards discontinuity. Hence, calculation of Nusselt number is based on cold wall. However, it could also have been calculated based on the energy balance at the partition wall.

RESULTS AND DISCUSSION

Figures 2, 3 and *4* describe the streamline maps and isotherm patterns for a partitioned cavity in which XH assumes values of 0.25, 0.5 and 0.75 respectively. The Rayleigh number (based on height) is 10^6 and the Prandtl number is assumed to be unity. The cavity aspect ratio is one and the partition is considered to be centrally located. The streamline patterns reveal that the streamlines are compressed in the region around the active portions of the hot wall. The fluid after receiving heat moves over the insulated portion of the vertical wall. The formation of a boundary layer is strongly dependent on the value of XH. While travelling over the insulated portion of the vertical wall, the streamlines diverge somewhat. This leads one to expect a near-quiescent pool at the top. This is particularly evident at lower values of XH, say XH = 0.25,

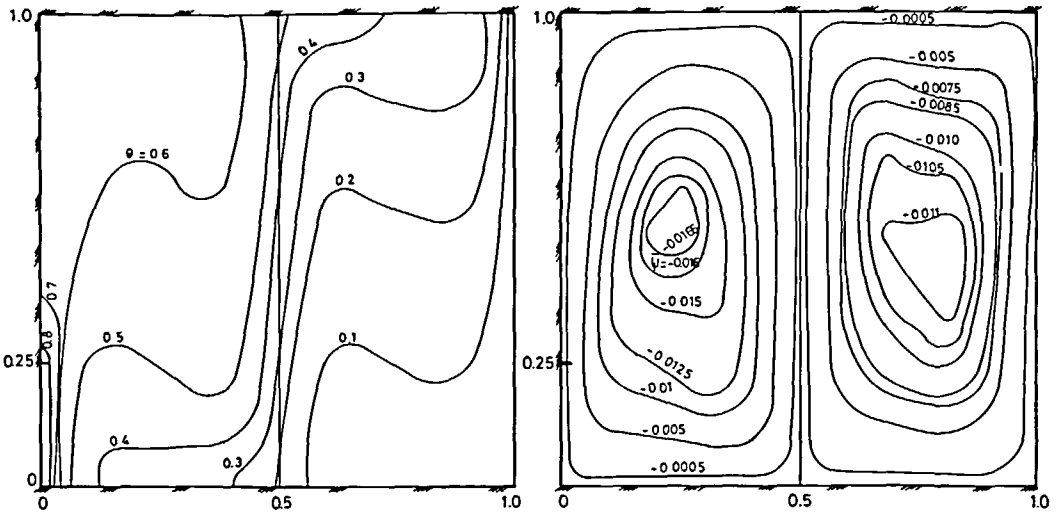

Figure 2 Isotherms and streamlines for XH = 0.25; $Ra_H = 10^6$, $Pr = 1$

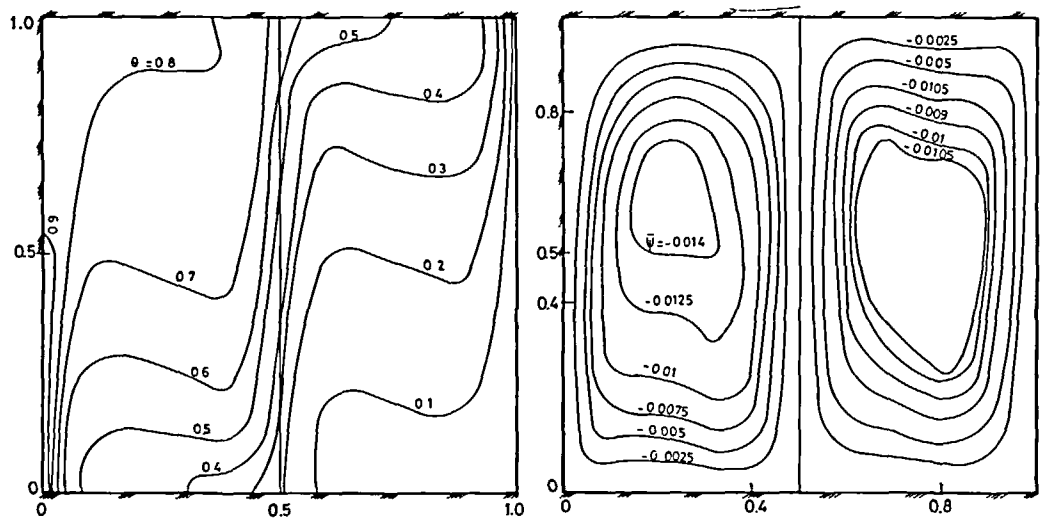

Figure 3 Isotherms and streamlines for XH = 0.5; $Ra_H = 10^6$; $Pr = 1$

where an isothermal pool with average non-dimensional temperature of 0.6 exists. It will be seen later that, with increase of XH, the isothermal pool gets replaced by a thermally stratified core. The flow while coming down along the partition exchanges heat with the fluid of the second chamber across the partition which is considered to be thermally thin. Hence, boundary layers are seen to exist throughout the length of the partition on either side of it. The available temperature differential across each chamber does not encourage formation of secondary cells in either of the chambers even when XH assumes a value of 0.75. However, the possibility of its existence is not ruled out when Ra_H is increased above 10^6. At this stage it is interesting to compare the present streamline maps with those of Reference 7. Similar studies were made with the exception that no partitions were considered. Otherwise, the flow parameters were the same.

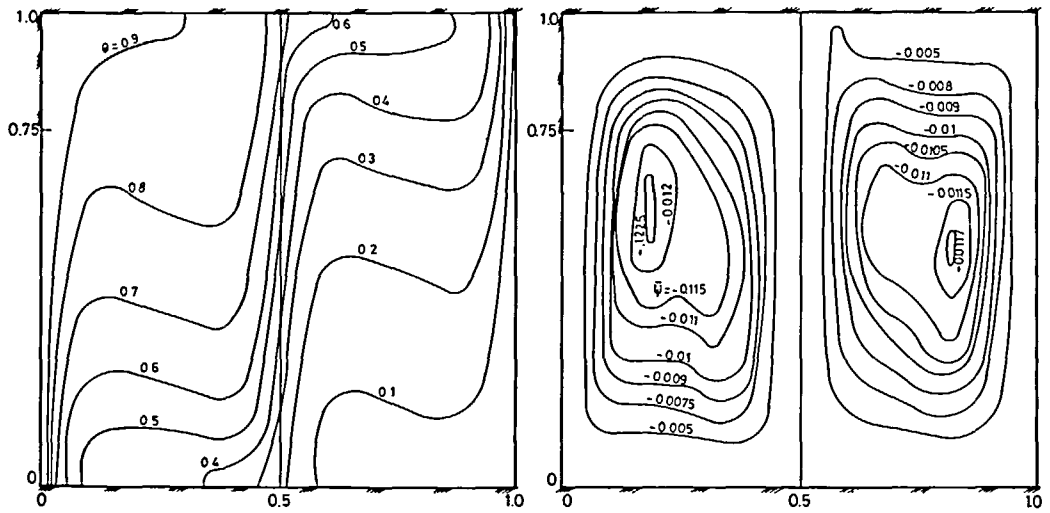

Figure 4 Isotherms and streamlines for XH=0.75; $Ra_H=10^6$; $Pr=1$

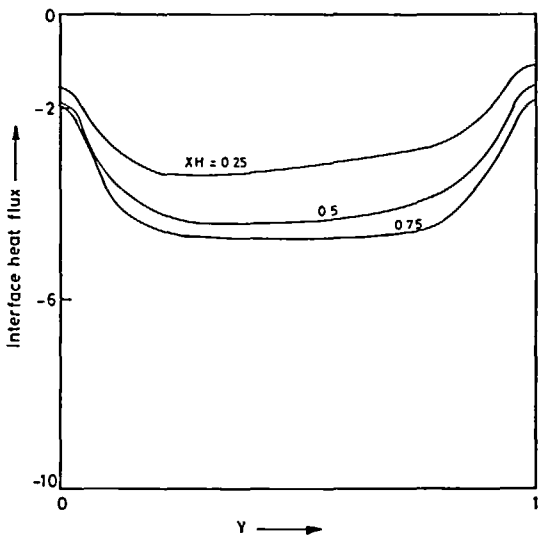

Figure 5 Variation of heat flux along the partition height with XH

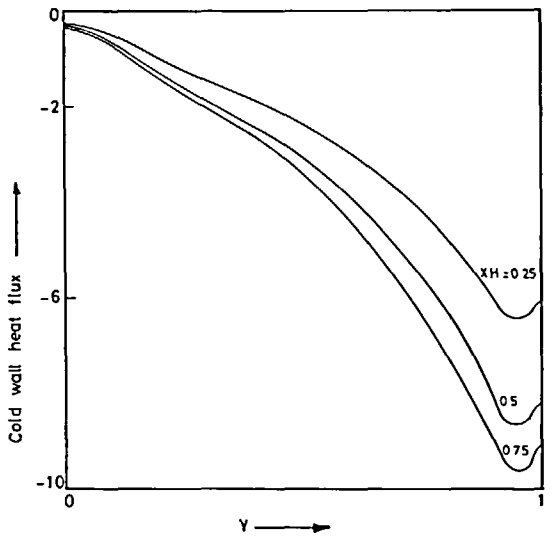

Figure 6 Variation of heat flux along cold wall with XH

We note[7] that for XH=0.25, there are no secondary cells while for XH=0.5 and 0.75, distinct secondary cells appear at different locations of the core. Also, with increasing XH, it is once again confirmed that the isothermal pool is replaced by a thermally stratified core.

Figure 5 depicts the variation of heat flux along the partition. The basic structure of all these curves is the same in the sense that minimum heat transfer occurs at the top and bottom of the partition. While a zone of near-constant heat flux distribution is obtained for XH=0.75, the one for XH=0.25 shows some deviation from it. Accordingly in *Figure 7*, for XH=0.75, the partition wall varies linearly for some distance along the height. This zone of near constant heat flux increases in width with increase of XH. *Figure 6* shows the variation of cold wall heat flux

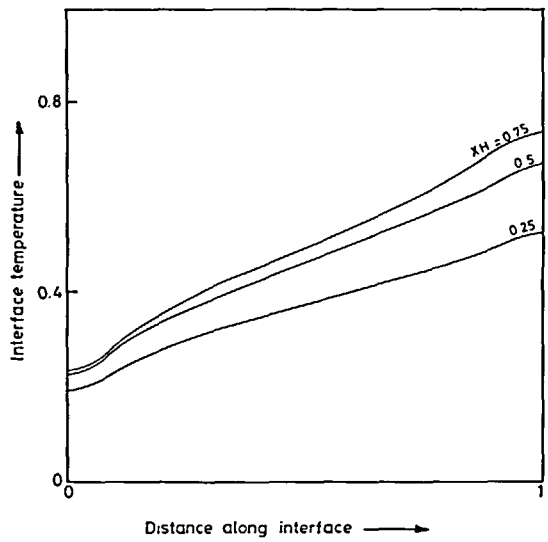

Figure 7 Variation of partition temperature with XH

for different values of XH. As expected, the heat flux increases from a minimum at the bottom to a maximum in the region around the cold corner; thereafter, heat flux decreases as one approaches the cold corner. The shape of isotherms near the cold corner provides an explanation of this behaviour. The compression of the isotherms due to the fluid motion around the corner results in a decrease of resistance to heat transfer. Hence maximum heat transfer occurs near the cold corner.

Tables 1 and *2* represent the computed Nusselt number values for various values of XH as well as for some other relevant configurations for which comparison can be made. The Nusselt number values for XH = 1 are taken from Reference 14. The quantities in parentheses indicate the average temperature of the partition wall. The quantities in brackets indicate the cold wall Nusselt number values for a square cavity having partially active heated side wall but without partition. For any given Rayleigh number, the Nusselt number increases with XH. Also as expected for any specified value of XH. The Nusselt number increases with Rayleigh number. However, it is also to be noted that the average partition temperature, after showing a steady increase in its value with Ra_H, drops somewhat at $Ra_H = 10^6$. The reason is not fully understood. *Table 2*, derived from Reference 12, shows the computed Nusselt number values for a square

Table 1 Computed values of the cold wall Nusselt numbers (Nu_C) for various values of Ra_H and XH

Ra_H	XH = 0.25	XH = 0.5	XH = 0.75	XH = 1 (without partition)
10^3	0.6226 (0.3122)	0.8222 (0.4116)	0.9538 (0.4766)	1.117
10^4	0.71473 (0.3382)	0.9678 (0.4367)	1.1023 (0.4847)	2.25
10^5	1.5236 (0.3704)	2.0246 (0.4593)	2.226 (0.4922)	4.601
10^6	2.8267 [4.494] (0.366)	3.7161 [6.956] (0.4556)	4.1395 [8.453] (0.4906)	9.02

Table 2 Computed values of cold wall Nusselt numbers when both the walls are fully active[12]

Ra_H	Nu_C (with centrally located partition)
10^3	1.0026
10^4	1.14
10^5	2.2782
10^6	4.292

cavity with centrally located partition when both the side walls are fully active. It is seen that while the effect of introducing the partition is to reduce the Nusselt number, the effect of mixed thermal conditions is to reduce it further.

CONCLUSION

A square cavity with centrally located partition and with a partially active side wall has been studied numerically. Flow structures reveal that at lower values of XH, convection is weak even at $Ra_H = 10^6$. The changes in thermal fields are also noted. The effect of partition as well as mixed thermal conditions is to reduce the overall heat transfer in the cavity.

NOMENCLATURE

x, y dimensional co-ordinates
X, Y non-dimensional co-ordinates
H height of cavity
W width of cavity
XP position of the partition
XH length of the active zone along heat zone
u, v horizontal and vertical components of velocity
U, Y non-dimensional velocity components
p, P dimensional and non-dimensional pressure
T temperature
Gr_H Grashof number (based on H) $\left[=\frac{\beta . g(T_W - T_C)H^3}{\nu^2}\right]$
Pr Prandtl number $(=\nu/\alpha)$
Ra_H Rayleigh number $(=Gr_H Pr)$
Nu_C Nusselt number at the cold wall $\left(=-\int_0^1 \left(\frac{\partial \theta}{\partial x}\right)_{x=1} dY\right)$
$T_{W,C}$ Hot and cold wall temperatures respectively
g Acceleration due to gravity

Greek symbols

ν kinetic viscosity
α thermal diffusivity
ρ density
θ non-dimensional temperature $\left(=\frac{T - T_C}{T_W - T_C}\right)$
β coefficient of volume expansion

REFERENCES

1 Ostrach, S. Natural convection in enclosures, *Advances in Heat Transfer*, Vol. 8, pp. 161–227, Academic Press, New York (1972)
2 de Vahl Davis, G. Natural convection of air in a square cavity: a benchmark solution, *Int. J. Num. Meth. Fluids*, **3**, 249–264 (1983)
3 Poulikakos, D. Natural convection in a confined fluid-filled space driven by a single vertical wall with warm and cold regions, *J. Heat Transfer, ASME*, **107**, 867–876 (1985)
4 November, M and Nansteel, M. W. Natural convection in rectangular enclosures heated from below and cooled from one side, *Int. J. Heat Mass Transfer*, **30**, 2433–2440 (1987)
5 Valencia, A and Frederick, R. L. Heat transfer in square cavities with partially active vertical walls, *Int. J. Heat Mass Transfer*, **32**(8), 1567–1574 (1989)

6 Sarkar, A. and Sastri, V. M. K. Finite element analysis of natural convection in the active corners of a square cavity, *Num. Heat Transfer*, in press
7 Ghosh, P. K., Sarker, A. and Sastri, V. M. K. Square cavity with partially active side walls—a finite element analysis, *Proc. 3rd ASME–JSME Joint Thermal Eng. Conf. (1991)*
8 Sparrow, E. M. and Prakash, C. Interaction between internal natural convection in an enclosure and an external natural convection boundary layer flow, *Int. J. Heat Mass Transfer*, **24**, 895–907 (1981)
9 Nishimura, T., Shiraishi, M. and Kawamura, Y. Analysis of natural convection heat transfer in enclosures divided by vertical partition plate, *Proc. Int. Symp. Heat Transfer, Beijing*, Paper No. 85-ISHT-I-6 (1985)
10 Acharya, S. and Tsang, C. H. Natural convection in a fully partitioned inclined enclosure, *Num. Heat Transfer*, **8**, 407–428 (1985)
11 Nishimura, T., Shiraishi, M., Nagasawa, F. and Kawamura, Y. Natural convection heat transfer in enclosures with multiple vertical partitions, *Int. J. Heat Mass Transfer*, **31**, 1679–1686 (1988)
12 Ghosh, P. K., Sarkar, A. and Sastri, V. M. K. Natural convection heat transfer in enclosure with partition, *Num. Heat Transfer*, to be published
13 Hood, P. Frontal solution program for unsymmetric matrices, *Int. J. Num. Meth. Eng.* **10**, 379–399 (1976)
14 Sarkar, A. and Sastri, V. M. K. Finite element solutions of steady, two dimensional natural convection equations, *Proc. Sixth Int. Conf. Num. Meth. Thermal Problems, Swansea*, pp. 1732–1742 (1989)